ELSEVIER

Biochimica et Biophysica Acta 1319 (1997) 59–68

BIOCHIMICA ET BIOPHYSICA ACTA
BBA

The photocycle of bacteriorhodopsin at high pH and ionic strength I. Effects of pH and buffer on the absorption kinetics

Géza I. Groma *, Roberto A. Bogomolni, Walther Stoeckenius

Department of Chemistry and Biochemistry, University of California, Santa Cruz, CA 95064, USA

Received 7 May 1996; accepted 12 September 1996

Abstract

A fitting analysis resolved the kinetics in the microsecond to second time range of the absorption changes in the bacteriorhodopsin photocycle at pH = 8.0–9.5 in 3 M KCl into seven exponential components. The time constants and/or amplitudes of all components are strongly pH-dependent. In the pH range studied, the logarithms of the pH-dependent time constants varied linearly with pH. The maximum absolute value of the corresponding slopes was 0.4, in contrast with the theoretically expected value of 1 for unidirectional reactions coupled directly to proton exchange with the bulk phase. This indicates that the extracted macroscopic rate constants are not identical to the microscopic rate constants for the elementary photocycle reaction steps. Unexpected differences were found in the kinetic parameters in CHES and borate buffers.

Keywords: Bacteriorhodopsin; pH; Photoselection; Anisotropy

1. Introduction

This paper presents an analysis of the kinetics of the bacteriorhodopsin (bR) photocycle at high pH and high ionic strength. Most earlier studies of this type [1–5] were carried out at low ionic strength. Experiments at high pH and high ionic strength [6–8], however, demonstrated that these conditions affect the photocycle kinetics, favoring accumulation of the intermediate N [9]. This slow-decaying species was shown to absorb maximally at around 560 nm. A slowly-decaying absorbance transient at around 410 nm also displayed high amplitudes at high pH and high salt concentration. This was earlier assigned to a thermal M-like intermediate generated from a photoreaction of N under continuous illumination [6]. In contrast, laser flash excitation of N did not yield any M-like photoproduct [10]. The existence of an M-like form among the photoproducts of N was later confirmed [11], but the above slowly-decaying M component was accounted for by introducing back-reactions in the photocycle [11–13]. The different interpretations of these kinetic transients were caused in part by the differences in the experimental conditions. These included measurement of the recovery kinetics after actinic illumination with different intensities, and of the flash-induced absorption kinetics with a chopped excitation and scanning spectrophotometer [6,7], an optical multichannel analyzer [12], or a resonance Raman kinetics technique [8]. These data

* Corresponding author. Present address: Institute of Biophysics, Biological Research Centre of Hungarian Academy of Sciences, 6726 Szeged, Hungary. Fax: +36 62433133; E-mail: groma@everx.szbk.u-szeged.hu

PII S0005-2728(96)00116-8

are directly comparable only for the simplest, unidirectional unbranching photocycle. In any other case, the relation between the microscopic rate parameters (characterizing a kinetic model) and the macroscopic rate parameters (i.e., the raw experimental data) will depend on the measurement conditions in a complex manner.

In addition to the above technical problem, kinetic analysis of the photocycle is further complicated by the growing evidence indicative of a real heterogeneity in the M population. For kinetic reasons, Váró and Lanyi introduced a model of two consecutive M forms [12] which were found to be spectroscopically distinguishable [14]. Their existence was interpreted as reflecting the two distinct states of an irreversible conformational switch, having a crucial role in the proton pumping mechanism [15]. Investigation of light-induced back-reactions from the thermally stabilized M state revealed that five different substates of this form exist [16]. The formation of M was found to be biphasic or multiphasic [17–21] and both the relative amplitude and the time constant of the slower phase exhibited a strong pH dependence above pH 8 [17,20]. These findings led to the idea of parallel photocycles originating from the amino acid residues having different protonation states and different proton pumping abilities [17–19,21]. This concept was supported by the recent observation of the pH dependence of the decay rate of the retinal photoexcited state [22].

The aim of the present study was to collect informative data at high ionic strength in the above critical pH range and to extract the microscopic rate constants. This first paper deals with a phenomenological description of the laser flash-induced kinetics in the microsecond-second time range at different pH and in the presence of different buffer materials. The following paper (this issue) characterizes the temporal changes in the anisotropy factor determined by photoselection and discusses possible models for the bR photocycle.

2. Materials and methods

The purple membrane of *Halobacterium salinarium* strain ET1001 was prepared by standard methods. The membrane fragments were immobilized in 15% polyacrylamide gel and soaked for at least 12 h in 3 M KCl buffered with 100 mM CHES or borate. The optical density of the samples at 570 nm was adjusted to 1. An 8×3 mm slab of the gel was cut and transferred with buffer solution to the thermostated (20°C) measuring cell.

Absorption kinetic measurements were made on a home-built instrument. The monitoring beam from a feedback-controlled Xe lamp (P.R.A. Vancouver, Canada) passed through a 0.25-m monochromator grating (Jarrel Ash, Metuchen, New Jersey) with a 15-nm bandpass and through a vertical polarizer, and was focused onto the 3-mm edge of the sample. The transmitted beam passed through a second identical monochromator and was detected with a photomultiplier (Hamamatsu R928). Its intensity was reduced until further reduction had a negligible effect on the kinetics. The sample was excited by a frequency-doubled YAG laser (Quanta Ray DCR-2, 532 nm, 4 ns). The partially polarized light of this laser passed first through a depolarizer and then through a polarizer mounted on a rotating frame. This exciting beam illuminated a 3-mm circular spot on the sample perpendicular to the monitoring beam. The energy of the laser at the sample was adjusted to 0.5 mJ before every measurement. A Nicolet 2090 digital oscilloscope (Nicolet, Madison, WI) equipped with a home-made quasi-logarithmic time base recorded the photomultiplier signal. This time base provided 32 blocks of 64 equidistant time points. The dwell time of the first block was 200 ns, which was doubled in every subsequent block. The second channel of the oscilloscope recorded a reference signal for every flash from the exciting laser, measured with a Molectron PM51002 (Portland, OR) energy-meter. Data acquisition was carried out with a program written in ASYST (Asyst Software Technologies, Inc., Rochester, New York) on an AT-286 microcomputer. All kinetics recorded with parallel and perpendicular polarization were averages of 200 scans. The repetition time was 15 or 30 s, depending on the recovery time of the photocycle. The quasi-logarithmic time base of the collected data was converted to true logarithmic. Typically 8 logarithmic points were generated within the 64 points of a linear block. The measured set of points from a particular block was filtered in frequency domain, using a Blackman window [23] with a cut-off frequency corresponding to 8

points, and a linear interpolation was then applied to generate logarithmically equidistant points. The first points, corrupted by the laser flash, were dropped before further analysis. Magic angle kinetics were calculated by using the formula:

$$A_M = (A_{par} + 2A_{perp})/3, \quad (1)$$

where A_M, A_{par} and A_{perp} denote the absorbance changes at the magic angle, and parallel and perpendicular to the excitation, respectively. It should be noted that simply setting the polarization at the magic angle during measurement of the absorbance changes can introduce errors [24]. The kinetic curves were analyzed by exponential fitting. The fitting program, written in FORTRAN, was based on the GLOBAL subroutine [25]. This routine was chosen in order to overcome the problem of the many local minima inherent in exponential fitting. Through a combination of a stochastic method for global optimization [26] with a Levenberg-Marquardt local search [27], the program proved very effective in reaching the true global minimum with high probability. A constant weighting factor for every data point was determined via estimation of the measurement error from the pretrigger parts of the traces. The fitting parameter errors were determined from the diagonal elements of the covariance matrix of the least square problem [27]. The program allowed the fitting of several kinetic traces recorded at different wavelengths both separately and simultaneously. In the latter case, the analysis required identical time constants for every wavelength. Conservation of material also required that the total sum of the amplitudes be zero at every wavelength. Thus the amplitude A_0 of an unresolved component is

$$A_0 = -(A_1 + A_2 + \ldots + A_n) \quad (2)$$

where A_i, $i = 1, \ldots, n$ is the amplitude of the ith component and n is the total number of components.

3. Results

The 415 nm absorption kinetics of bR at high pH is usually described as comprising two components in both rise and decay. The high information content of the kinetic data taken in a logarithmic time base and the sophisticated fitting procedure of the GLOBAL subroutine made it possible to explore the finer details of the kinetics. In the first step of our analysis, we determined the number of first-order reactions necessary and sufficient to describe the experimental data. As an example, Fig. 1 depicts the simultaneous fitting of the 415 and 550 nm kinetics with three to seven exponential components for CHES buffer at pH = 9.0. The result of visual comparison of the measured and calculated curves can be considered satisfactory, even with four components. The residuals, however, exhibit a definite structure, which vanishes only when seven components are used. Fig. 2 shows graphically the time constants and the amplitudes corresponding to the fittings. The values of the time constants are well separated and their uncertainties (represented by horizontal error bars) are negligible. This argues strongly in favor of discrete first-order reactions and against the possibility of distributed kinetics. In the latter case, the uncertainties in the time constants would be expected to be comparable to their differences in absolute values. Stepping from six to seven components changes neither the time constants nor the amplitudes of the first five components. Neglect of the seventh component of relatively low weight, however, markedly changes the position of the sixth.

Fig. 2F supports the importance of all seven exponentials for a complete description of the experimental data. It represents the result of separate fitting of the kinetics at 415 and 550 nm with six components. The results demonstrate that practical identity of the time constants at the two wavelengths is satisfied for four components. However, there is no counterpart for the fourth component at 415 nm and only one low-weight counterpart for the last two components at 550 nm. Fig. 2E reveals that the missing components have very low amplitudes. Because of this, it was not possible to fit the kinetics separately with seven exponentials. At the same time, the counterparts of the above critical time constants are of high weight, indicating that all of them are actually necessary to describe the kinetics at these two wavelengths. This concept is supported by the statistical parameters corresponding to the distribution of the residuals of fits. A plot of their standard deviation against the number of exponentials (Fig. 3) indicates a definite decrease, even in the last step. *F*-test

calculations [27] resulted in a very low ($<10^{-5}$) probability of the null hypothesis that the residuals corresponding to the fitting with six and seven exponentials have identical distribution. Consequently, such a hypothesis should be rejected, validating the existence of seven true components in the data. A statement that these seven components are also sufficient for a complete description of the kinetics is much less obvious. The decrease of the standard deviation points to definite, but incomplete saturation at seven exponentials. The program we used failed to find an eighth component by simultaneous fitting. A typical result of such a trial was the appearance of two components with very close time constants, and unusually high amplitudes with opposite signs (see also Refs. [1,2]). Since all known intermediates of the bR photocycle exhibit considerable absorbance at 415 and/or 550 nm, it is very unlike that kinetic measurements at other wavelengths could introduce a new component in the data, but this possibility cannot be completely excluded.

After determining the correct number of compo-

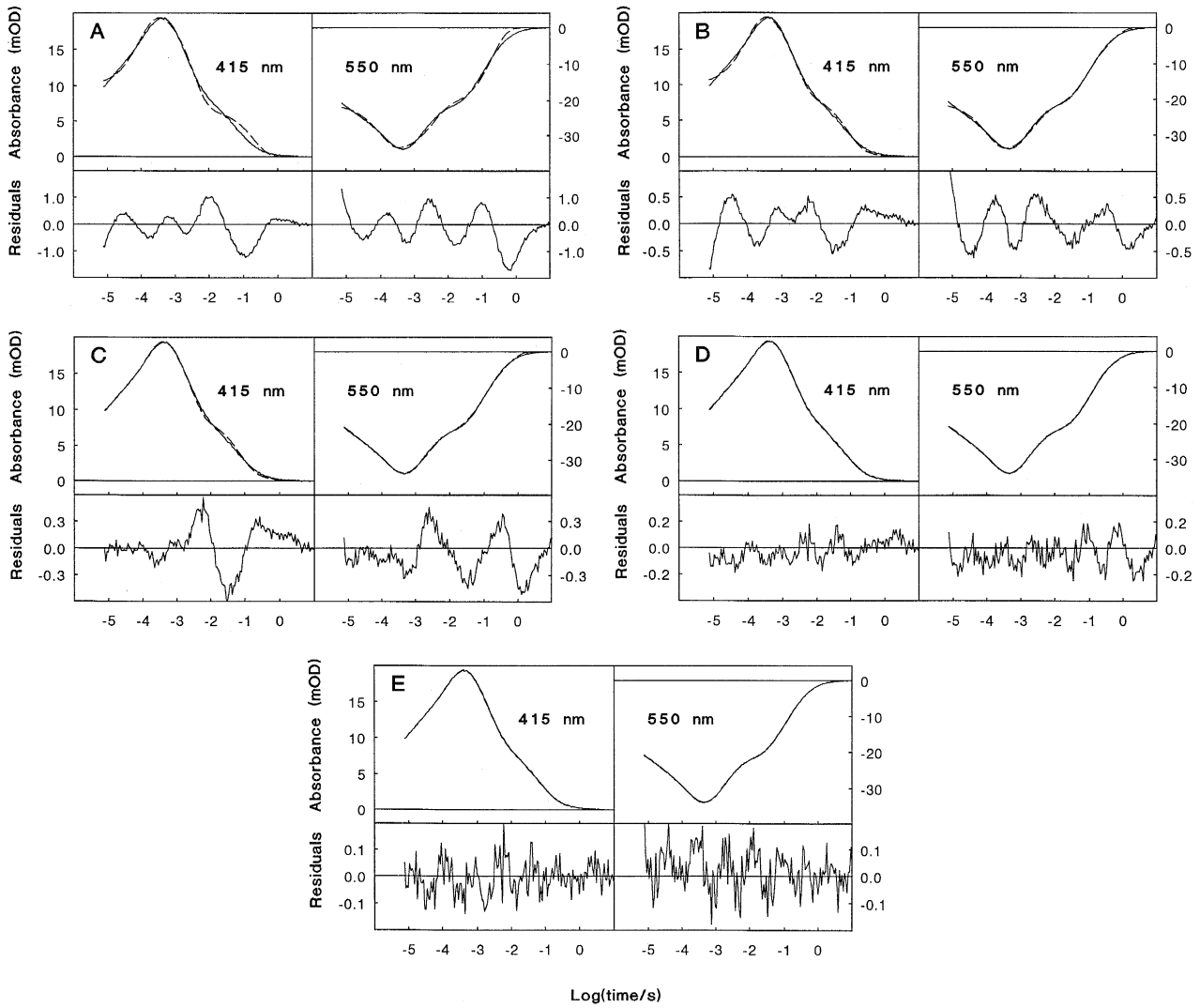

Fig. 1. Fitting series of flash-induced absorption kinetics data. Solid line: Experimental data in 3 M KCl and 100 mM CHES buffer (pH = 9.0). Magic angle kinetics calculated via Eq. (1) from parallel and perpendicular polarization. Dashed line: fitting curves of (A) three, (B) four, (C) five, (D) six and (E) seven exponentials. Fitting was carried out simultaneously at 415 and 550 nm. Lower curves: magnified residuals (experimental minus fitted data).

nents, we used their parameters to characterize the kinetics at different pH values. Fig. 4 illustrates the pH dependence of the time constants in CHES and borate buffers. In the pH range studied, the time constants were either pH-independent or displayed a linear dependence on proton concentration. If a given step of the photocycle represents a pure proton uptake or release process, a slope of 1 or −1, respectively, is to be expected for this pH dependence (see Section 4). The fact that all the slopes have a much lower absolute value is a strong indication that the observed macroscopic rate constants reflect not ele-

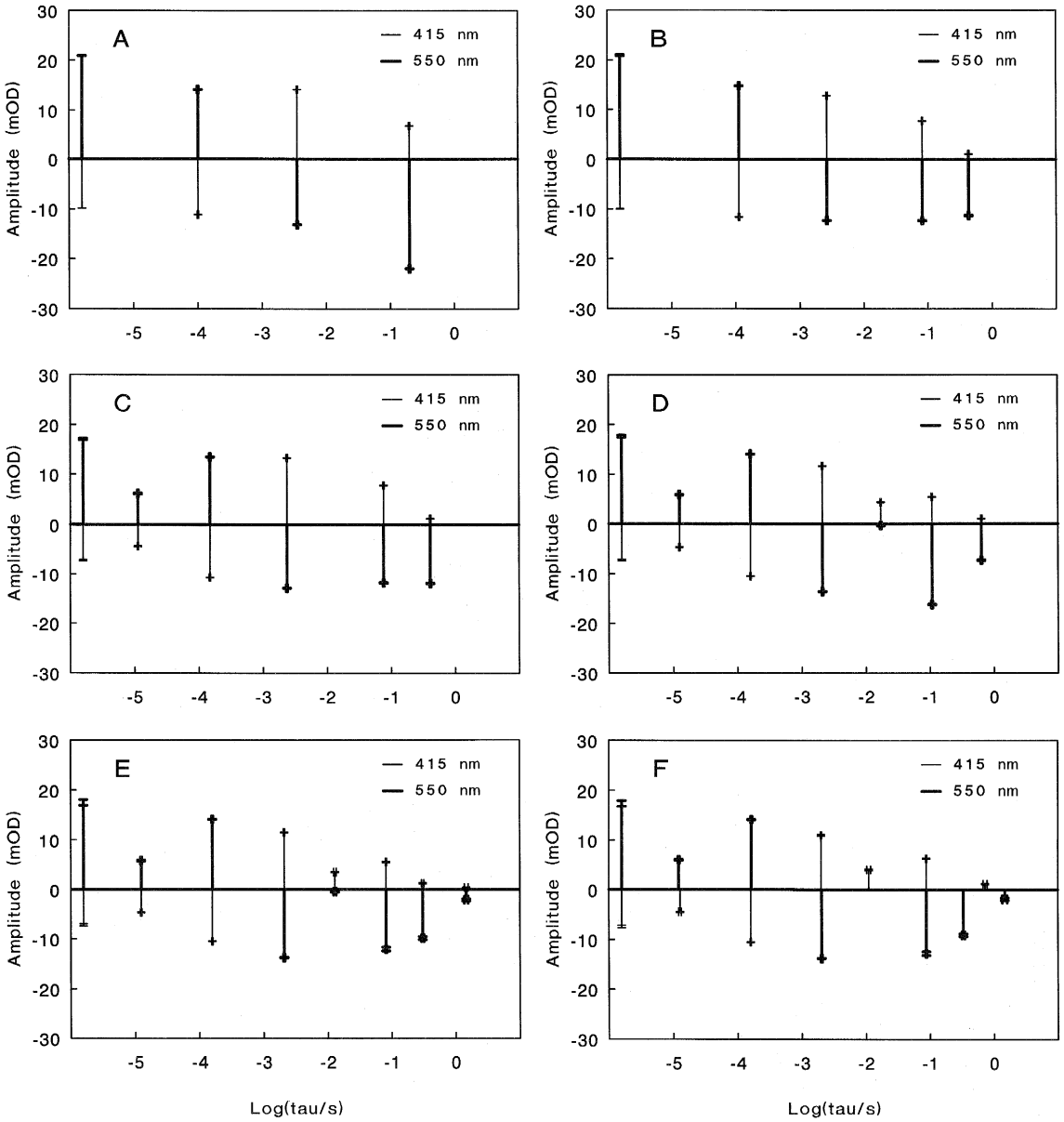

Fig. 2. Graphical representation of the fitting parameters presented in Fig. 1. The horizontal position and the height of each bar (with positive or negative sign) correspond to the time constant and the amplitude of a fitting exponential, respectively. The left-most bar represents the unresolved component calculated via Eq. (2); its position does not yield any information. The horizontal and vertical error bars correspond to the error in the time constant and the amplitude, respectively. Results of simultaneous fitting at 415 and 550 nm with (A) three, (B) four, (C) five, (D) six and (E) seven exponentials. (F) Results of separate fitting with six exponentials.

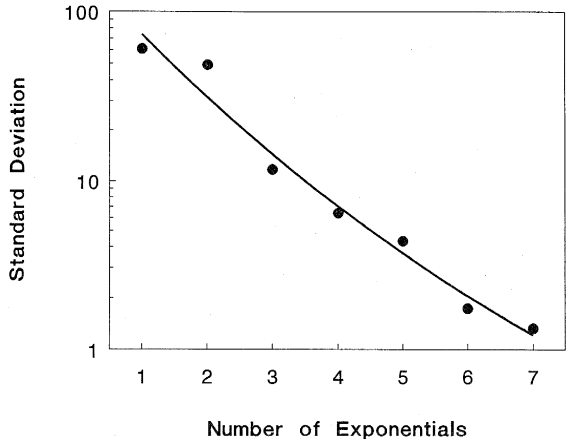

Fig. 3. Dependence of the standard deviation of fitting on the number of exponentials. The continuous line is drawn only to lead the eye.

mentary reaction constants, but some combination of them. Unexpectedly, the slopes of the components C4 and C7 are very different in the CHES and the borate buffers. Fig. 5 shows the pH dependences of the amplitudes for the different exponential components in the two buffer solutions. In contrast with the time constants, a linear dependence is not expected for the amplitudes, even for the simplest scheme of the photocycle, and any quantitative analysis is possible only in the framework of a particular kinetic model. This type of analysis will be presented in a later paper. Even without it, however, the following qualitative conclusions can be drawn:

(i) The majority of the amplitudes are strongly pH-dependent.

(ii) The amplitudes of C0, C1 and C2 are negative at 415 nm. Loosely speaking, they represent 'M rise' processes. These amplitudes and the corresponding time constants reveal minor buffer effects.

(iii) In contrast with the former processes, the 'M decay' components C3–C7 exhibit a pronounced and complex buffer dependence. One of the major amplitudes, C3, has a much higher absolute value in CHES than in borate. At the same time, C6 and C7 have small amplitudes in CHES, but markedly higher amplitudes in borate, which results in an overall slowing down of the photocycle in the borate buffer. To exclude an error due to differences in the samples, we exchanged the buffers in the gel slabs. The kinetics showed the characteristics of the buffer present. However, when we repeated the measurements with several different samples, we found variations in the extent of the difference between the kinetics in the two buffers, which we are unable to explain so far.

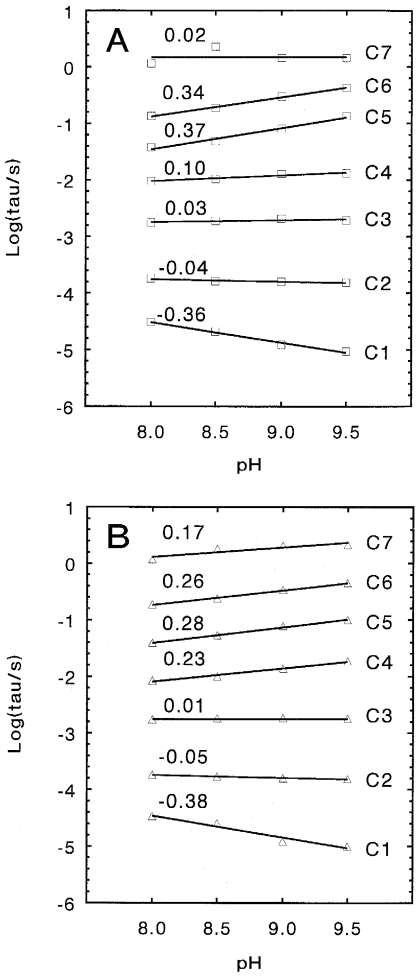

Fig. 4. pH dependences of the time constants of the seven fitting exponentials in (A) CHES and (B) borate buffer. The numbers above the fitted linear plots indicate their slopes.

Fig. 5. pH dependences of the amplitudes corresponding to rates C1–C7 in Fig. 4. C0 represents the amplitude of the unresolved component. Squares with dashed lines correspond to CHES buffer, and triangles with solid lines to borate buffer.

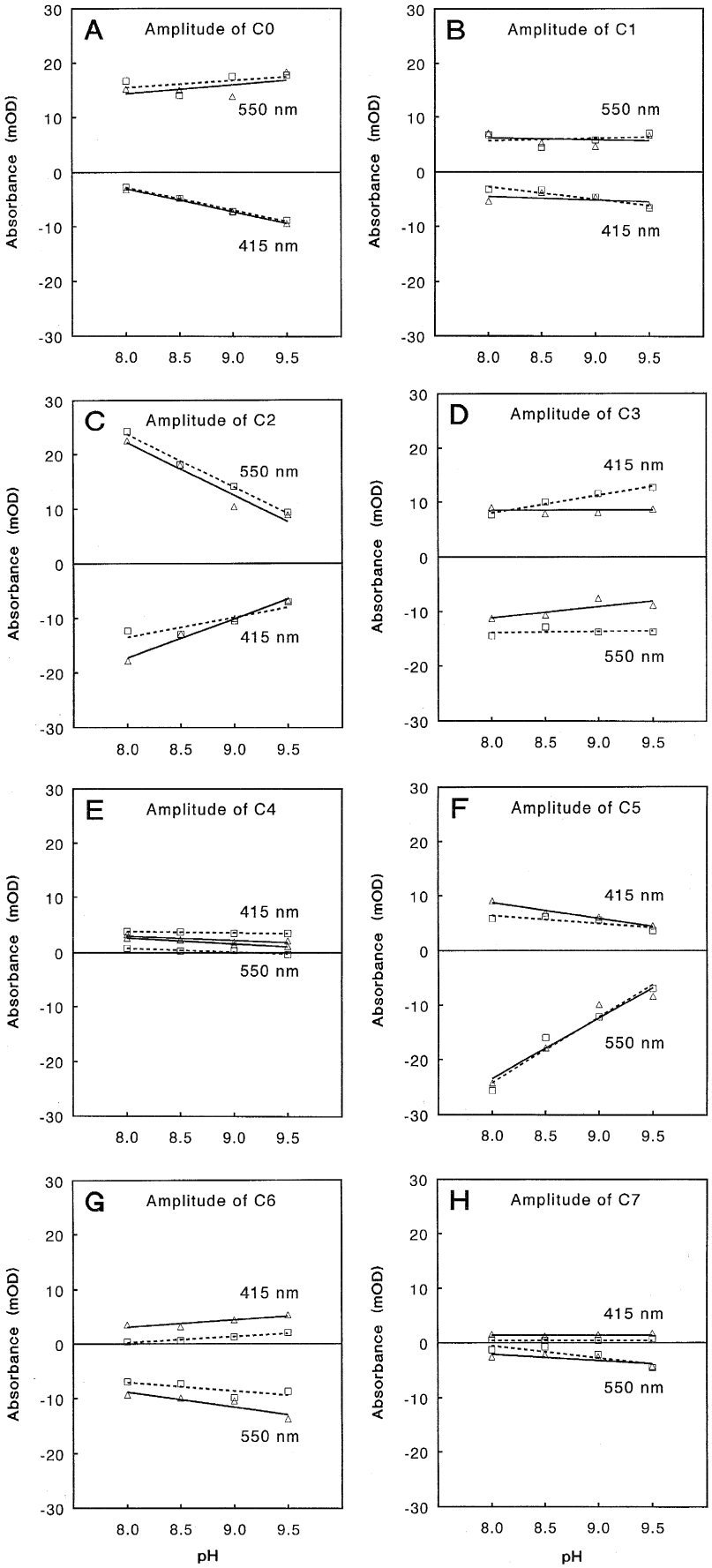
A
Amplitude of C0
550 nm
415 nm
B
Amplitude of C1
550 nm
415 nm
C
Amplitude of C2
550 nm
415 nm
D
Amplitude of C3
415 nm
550 nm
E
Amplitude of C4
415 nm
550 nm
F
Amplitude of C5
415 nm
550 nm
G
Amplitude of C6
415 nm
550 nm
H
Amplitude of C7
415 nm
550 nm
Absorbance (mOD)
pH
30
20
10
0
-10
-20
-30
8.0
8.5
9.0
9.5

4. Discussion

The results described demonstrate that at high pH and high ionic strength seven (macroscopic) first-order processes are necessary and probably sufficient to characterize the absorption kinetics of the photocycle after the formation of the L intermediate(s). According to the theory of first-order reactions, this requires the existence of seven intermediates (including L, but not the terminating bR form), regardless of the number of transitions between them [9]. In contrast, the traditional model of the photocycle involves only four intermediates (L, M, N and O) in this time region. This model, however, is based on data taken at around neutral pH and at low ionic strength [3–5]. Xie and co-workers [2] recently collected a dataset in the pH range 5–9 at different temperatures and wavelengths. They too found that seven exponentials are necessary to describe the L to bR kinetics. The macroscopic time constants determined from their data at pH = 9.0 and 20°C are compared with our values at pH = 8.0 and 9.0 in Table 1. The fastest kinetic component reported by Xie et al. corresponds to the K-L transition, and hence no corresponding counterpart is found in our data. The next three time constants, however, display good correlations. The last three components of Xie et al. are 2–3 times faster than ours. No counterpart is found corresponding to our two extremely slow components. The main difference in the experiments is the ionic composition. Xie et al. used 10 mM NaCl, while our experiments were carried out in 3 M KCl. At low ionic strength, the local pH at the membrane surface is considerably lower than in the bulk solution [28], whereas in 3 M salt the two values should be practically identical. This may explain the differences found for several time constants. For components C1 and C5, which display a strong pH dependence, this difference is less if the data obtained at pH = 9.0 by Xie at al. are compared to ours at pH = 8.0 (Table 1). It is worth noting here that, besides local pH effects, the protein conformation and other molecular properties may be affected by ionic strength.

Table 1
Comparison of our data with time constants determined by Xie et al. [2] from their Fig. 6C: pH = 9.0, T = 20°C, ionic strength = 10 mM Na^+; our data from Fig. 4A: pH = 8.0 and pH = 9.0, T = 20°C, ionic strength = 3.0 M K^+

	Time constants (ms)		
	Xie et al.	This study	
	pH = 9.0	pH = 8.0	pH = 9.0
	0.002	–	–
C1	0.05	0.03	0.01
C2	0.2	0.2	0.2
C3	2	2	2
	3	–	–
C4	20	10	10
C5	50	40	80
C6	–	100	300
C7	–	1000	1000

For all the macroscopic rate constants, the pH dependence was found to be linear on a logarithmic rate constant scale, and the absolute value of the highest slope was < 0.4. It should be 1, however, for a pure, unidirectional protonation/deprotonation reaction. If a second order reaction is assumed:

$$X^- + H^+ \underset{k_{-1}}{\overset{k_1}{\Leftrightarrow}} XH$$

$k_{app} = [H^+]^* k_1 + k_{-1}$ will be an apparent (pseudo) first-order rate constant. If the reverse reaction has a negligible rate, the pH dependence of $|\log(k_{app})|$ will have a slope of 1. Clearly, if the reverse reaction must also be taken into account, the slope will be lower.

Kouyama et al. [6,7] analyzed the rate constants in the same pH range as we worked in, and found a slope of 0.8–0.9 for the N decay, one of 0.6–0.7 for the slow M decay and a small negative slope for the fast M decay. These values differ considerably from ours. It is difficult to compare the data, however, because Kouyama et al. [6] used different experimental conditions to determine the three rate constants. They followed the recovery kinetics at 580 nm after a weak illumination to determine the rate constant for the N decay, whereas the rate constant of the slow M decay was determined from the kinetics at 410 nm after a strong actinic illumination. Finally, the fast M kinetics was determined from the response to a short flash. Theoretically, these techniques should yield the same macroscopic rate constants. However, the amplitudes of the different components depend strongly on the initial conditions. The weights of the slow components are generally much higher in a response to the turning-off of a constant actinic light than in

response to a short flash. Use of the former type of experiment and a linear time base will lead only to a first approximation of the overall rate constant corresponding to a weighted mixture of the slow processes.

Since we determined all the macroscopic rate constants from laser flash experiments with use of a logarithmic time base, and applied a constraint of identical rate constants for 415 and 550 nm in the course of the analysis, we were able to obtain more detailed information about the individual kinetic components. The fact that the slopes of the pH dependences of the rate constants deviate markedly from unity strongly indicates that the macroscopic rate constants themselves do not represent elementary reaction steps. The theoretical pH dependence with a slope of unity holds for microscopic rate constants only, and the macroscopic constants can differ widely from this. A good example of this phenomenon is presented by Otto et al. [29], who studied the M decay in a wide pH range. On fitting the decay kinetics with two components, they found that the slope of the slower one varied continuously from 0 to 1 in the pH range 7–10. In their model, it was presumed that the Schiff base is reprotonated by an internal donor in the M → N transition and that the donor is reprotonated by the bulk aqueous phase during the decay of the N form. When an N → M back-reaction was included, this relatively simple model reproduced the above pH dependence of the slow component in the M decay very well. In the pH range 8.0–9.5, where our experiments were carried out, the data of Otto et al. yield a value of 0.6 for the average slope of this component (see Fig. 1 in Ref. [29]). This is far from the value of 1 expected for a pure proton-uptake process, but higher than the maximum slope of 0.4 represented by components C5 and C6 describing M-like decays in our analysis (Fig. 4). One reason for this difference could be the higher ionic strength we used. Another, and probably more important, reason is that our analysis supposes much more details in the structure of the photocycle kinetics. Consequently, the pH dependences of the apparent (macroscopic) rate constants can deviate more from those for pure proton-exchange processes. A detailed study of the relation of the microscopic and macroscopic rate constants for our data will be presented in a later paper.

Even in the absence of a detailed kinetic model of the bR photocycle under the studied conditions, the pH dependences of the macroscopic kinetic parameters provide useful information. One important point is the multiphasic nature of the rising kinetics of the M-like intermediates observed in the pH range we applied [17–21]. An earlier study demonstrated that in the interval between pH = 8 and 11 this rise can be decomposed into three components, having pH-independent time constants of 0.4 μs, 6 μs and 85 μs, respectively [30]. With increasing pH, the relative weights of the first two components increased at the expense of the third one. This tendency is clear in our data, too. Here, the 0.4 μs and 6 μs components are represented as unresolved ones (Fig. 5A), and the 85 μs component is probably identical to our C2 transition (Fig. 4, Fig. 5C, and Table 1). The time constant of C2 is pH-independent, and its amplitude is negative (representing rise) at 415 nm, with decreasing absolute value at increasing pH. The somewhat higher time constant (200 μs) can be attributed either to the higher ionic strength or to the larger number of components (mainly the existence of C1) in our analysis. Such a pH-dependent weight was interpreted by Balashov et al. [19] as the coexistence of a 'normal' and an 'alkaline' form of bR, both forms having their own photocycle. In this model, the 'alkaline' branch is attributed to the protonation of an amino acid residue (probably tyrosine) with intrinsic pK ≈ 8.3. In 3 M KCl this should be roughly equal to the effective pK (see above), and therefore the intermediates of the 'alkaline' photocycle should be represented in our data. The above-mentioned problem of the unknown microscopic kinetic parameters and the lack of detailed spectral information does not allow the different components to be sorted into the two branches. Additionally, in the studied pH range a minor contribution of the very alkaline form of bR, characterized by an absorption maximum at around 460–480 nm [19,31], cannot be completely excluded. Nevertheless, on the basis of the pronounced decrease in their weight with increasing pH, C2 (M-like rise) and C5 (M-like decay) clearly correspond in the framework of this model to the photocycle of the 'normal' bR form.

An unexpected result of our experiments is the marked dependence of the kinetic parameters on the buffer material used. This indicates a direct interac-

tion of the buffer molecules with bR, causing changes in the late phase of its kinetics. An effect of buffer molecules on the kinetics of the microsecond photocurrent component of bR has recently been reported [32]. It was explained by the movement of charged buffer molecules upon protonation. This effect was not manifested in the optical signals and disappeared at high salt concentration, and hence it has no direct relation to our observation. Even so a similar mechanism could also be involved under our experimental conditions.

Acknowledgements

We thank Dr. J. Fukushima for a critical reading of the manuscript. This work was supported by National Institute of Health Program Project Grant GM-27507 (W.S. and R.A.B.), NSF Grant DBM-8717193 (R.A.B.), NIH Grant GM-43561 (R.A.B.) and National Scientific Research Foundation of Hungary Grants OTKA T914 and T6401 (G.I.G.).

References

[1] Nagle, J.F., Parodi, L.A. and Lozier, R.H. (1982) Biophys. J. 38, 161–174.
[2] Xie, A.H., Nagle, J.F. and Lozier, R.H. (1987) Biophys. J. 51, 627–635.
[3] (a) Maurer, R., Vogel, J. and Schneider, S. (1987) Photochem. Photobiol. 46, 247–253. (b) Maurer, R., Vogel, J. and Schneider, S. (1987) Photochem. Photobiol. 46, 255–261.
[4] Müller, K.-H. and Plesser, Th. (1991) Eur. Biophys. J. 19, 231– 240.
[5] Müller, K.-H., Butt, H.J., Bamberg, E. Fendler, K. Hess, B. Siebert, F. and Engelhard, M. (1991) Eur. Biophys. J. 19, 241–251.
[6] Kouyama, T., Nasuda-Kouyama, A. Ikegami, A. Mathew, M.K. and Stoeckenius, W. (1988) Biochemistry 27, 5855–5863.
[7] Kouyama, T. and Nasuda-Kouyama, A. (1989) Biochemistry 28, 5963– 5970.
[8] Fodor, S.P., Ames, J.B., Gebhard, R. Van der Berg, E.M. Stoeckenius, W., Lugtenburg, J. and Mathies, R.A. (1988) Biochemistry 27, 7097–7101.
[9] Lozier, R.H. and Niederberger, W. (1977) Fed. Proc. 36, 1805–1809.
[10] Drachev, L.A., Kaulen, A.D., Skulachev, V.P. and Zorina, V.V. (1986) FEBS Lett. 209, 316–320.
[11] Brown, L.S., Zimányi, L., Needleman, R., Ottolenghi, M. and Lanyi, J.K. (1993) Biochemistry 32, 7679–7685.
[12] Váró, G. and Lanyi, J.K. (1990) Biochemistry 29, 2241–2250.
[13] Lozier, R.H., Xie, A., Hofrichter, J. and Clore, M. (1992) Proc. Natl. Acad. Sci. USA 89, 3610–3614.
[14] Váró, G. and Lanyi, J.K. (1991) Biochemistry 30, 5008–5015.
[15] Váró, G. and Lanyi, J.K. (1991) Biochemistry 30, 5016–5022.
[16] Friedman, N., Gat, Y., Sheves, M. and Ottolenghi, M. (1994) Biochemistry 33, 14758–14767.
[17] Hanamoto, J.H., Dupuis, J.P. and El-Sayed, M.A. (1984) Proc. Natl. Acad. Sci. USA 81, 7083–7087.
[18] Diller, R. and Stockburger, M. (1988) Biochemistry 27, 7641–7651.
[19] Balashov, S.P., Govindjee, R. and Ebrey, T.G. (1991) Biophys. J. 60, 475–490.
[20] Lin, G.C., Awad, E.S. and El-Sayed, M.A. (1991) J. Phys. Chem. 95, 10442–10447.
[21] Drachev. L.A., Kaulen, A.D. and Komrakov, A.Yu. (1992) FEBS Lett. 313, 248–250.
[22] Song, L., Logunov, S.L., Yang, D. and El-Sayed, M.A. (1994) Biophys. J. 67, 2008–2012.
[23] Blackman, R.B. and Tukey, J.W. (1958) The measurement of power spectra, Dover.
[24] Lewis, J.W. and Kliger, D.S. (1991) Photochem. Photobiol. 54, 963–968.
[25] Csendes, T., B. Daroczy, and Z. Hantos, (1985) in System Modelling and Optimization (Pekopa, A., Szelezsan, J. and Strazicky, B. Berlin, eds.), Vol. 84, Springer, Berlin, pp. 188–192.
[26] Boedner, C.G.E., Rinnooy Kan, A.H.G., Timmer, G.T. and Stougie, L. (1982) Math. Prog. 22, 125–140.
[27] Press, W.H., Flannery, B.P., Teukolsky, S.A. and Vetterling, W.T. (1988) Numerical recipes in C. Cambridge University Press, Cambridge, pp. 471–565.
[28] Szundi, I. and Stoeckenius, W. (1989) Biophys. J. 56, 369–383.
[29] Otto, H., Marti, T., Holz, M., Mogi, T., Lindau, M., Khorana, H.G. and Heyn, M.P. (1989) Proc. Natl. Acad. Sci. USA 86, 9228–9232.
[30] Liu, S.Y. (1990) Biophys. J. 57, 943–950.
[31] Druckmann, S., Ottolenghi, M., Pande, A., Pande, J. and Callender, R.H. (1982) Biochemistry 21, 4953–4959.
[32] Liu, S.Y., Kono, M. and Ebrey, T.G. (1991) Biophys. J. 60, 204–216.